



## Left ventricular endocardial longitudinal and transverse changes during isovolumic contraction and relaxation: a challenge

Wolfgang A. Goetz, Emmanuel Lansac, Hou-Sen Lim, Patricia A. Weber and Carlos M. G. Duran

*AJP - Heart* 289:196-201, 2005. First published Feb 11, 2005; doi:10.1152/ajpheart.00867.2004

### You might find this additional information useful...

---

This article cites 33 articles, 12 of which you can access free at:

<http://ajpheart.physiology.org/cgi/content/full/289/1/H196#BIBL>

Updated information and services including high-resolution figures, can be found at:

<http://ajpheart.physiology.org/cgi/content/full/289/1/H196>

Additional material and information about *AJP - Heart and Circulatory Physiology* can be found at:

<http://www.the-aps.org/publications/ajpheart>

---

This information is current as of June 27, 2005 .



## Left ventricular endocardial longitudinal and transverse changes during isovolumic contraction and relaxation: a challenge

Wolfgang A. Goetz, Emmanuel Lansac, Hou-Sen Lim, Patricia A. Weber, and Carlos M. G. Duran

The International Heart Institute of Montana Foundation, St. Patrick Hospital and Health Sciences Center and The University of Montana, Missoula, Montana

Submitted 24 August 2004; accepted in final form 17 January 2005

**Goetz, Wolfgang A., Emmanuel Lansac, Hou-Sen Lim, Patricia A. Weber, and Carlos M. G. Duran.** Left ventricular endocardial longitudinal and transverse changes during isovolumic contraction and relaxation: a challenge. *Am J Physiol Heart Circ Physiol* 289: H196–H201, 2005. First published February 11, 2005; doi:10.1152/ajpheart.00867.2004.—Left ventricular (LV) longitudinal and transverse geometric changes during isovolumic contraction and relaxation are still controversial. This confusion is compounded by traditional definitions of these phases of the cardiac cycle. High-resolution sonomicrometry studies might clarify these issues. Crystals were implanted in six sheep at the LV apex, fibrous trigones, lateral and posterior mitral annulus, base of the aortic right coronary sinus, anterior and septal endocardial wall, papillary muscle tips, and edge of the anterior and posterior mitral leaflets. Changes in distances were time related to LV and aortic pressures and to mitral valve opening. At the beginning of isovolumic contraction, while the mitral valve was still open, the LV endocardial transverse diameter started to shorten while the endocardial longitudinal diameter increased. During isovolumic relaxation, while the mitral valve was closed, LV transverse diameter started to increase while the longitudinal diameter continued to decrease. These findings are inconsistent with the classic definitions of the phases of the cardiac cycle.

mitral valve; ventricles; hemodynamics; isovolumic contraction; isovolumic relaxation; mitral valve closure; cardiac cycle phases; left ventricle diameters

THE CARDIAC CYCLE IS TRADITIONALLY divided into isovolumic contraction (IVC), ejection, isovolumic relaxation (IVR), and diastole (7). The concept of an initial isometric contraction during ventricular systole was originated by Wiggers (32), who stated that the first elevation in intraventricular pressure closes the atrioventricular valves while the ventricles contract in an isometric fashion. During the interval between the beginning of the rise in intraventricular pressure and the opening of the semilunar valves, the ventricular cavities are completely enclosed with a rising tension without change in ventricular volume. Later, Rushmer (23) showed that the initial phase of contraction was not an isometric contraction of all myocardial fibers of the left ventricle (LV). During IVC, he observed a rapid increase in LV pressure, a fast expansion of LV external circumference, and a rapid shortening of LV internal length. His conclusions were drawn from two experiments where he could successfully place internal distance gauges. In all other experiments, he failed to demonstrate the initial shortening of internal longitudinal dimension during IVC. Nevertheless, he concluded that the LV abruptly shortens during IVC and that this shortening is accompanied by an outward bulging of the

LV main body (24, 26). This sphericity of the external LV during IVC has also been described by several investigators (9, 27), who, in most cases, used epicardial markers. Others demonstrated the opposite, i.e., an elliptical pattern due to shortening of the LV internal minor axis (10, 19) and lengthening of its major axis diameters (27). This apparent discordance is probably due to the different behavior of the external (epicardial) and internal (endocardial) location of the markers.

Rankin et al. (20) found that the pattern of LV contraction was a function of its volume. The IVC pattern in the open-chest, hypovolumic dog was spherical but could reverse to an elliptical shape under normovolumic conditions.

During IVR, the LV internal geometric pattern has not been systematically evaluated. Rankin et al. (20) briefly mentioned a more spherical shape of the LV during IVR, and Nikolic et al. (18) and Lynch and Bove (16) described a more elliptical configuration.

The changes in LV longitudinal and transverse diameters during the two isovolumic phases of the cardiac cycle have not been precisely described in terms of quantitative geometric changes and their time sequence.

The purpose of this project was to use sonomicrometry to study the LV geometric changes during each phase of the cardiac cycle. We chose to study the opening and closing of the mitral valve because it has been used to define the different phases of the cardiac cycle. A simultaneous study of the aortic valve (although desirable) was not done because the number of available crystals was limited and because we had sonomicrometric data on this valve (13).

### METHODS

Six adult Targhee sheep ( $58 \pm 18$  kg; Sherick Farm, Missoula, MT) were implanted with 13 ultrasonic crystals via a cardiopulmonary bypass. After the animals were weaned from bypass and the pericardial sac was closed, recordings were obtained under stable hemodynamic conditions.

All animals received humane care in accordance with the *Principles of Laboratory Animal Care*, formulated by the Animal Welfare Act in the National Institutes of Health (NIH) *Guide for Care and Use of Laboratory Animals* [DHHS Pub. No. (NIH) 85-23, Revised 1996]. The protocol for the use of these animals for this research was also reviewed and approved by the Institutional Animal Care and Use Committee of The University of Montana.

**Surgical protocol.** The sheep were premedicated with ketamine (1.0 mg/kg) and propofol (4.0 mg/kg). Artificial ventilation was achieved using a volume-regulated respirator (North American Drager, Telford, PA). Electrocardiogram was monitored continuously

Address for reprint requests and other correspondence: C. M. G. Duran, The International Heart Institute of Montana, 554 West Broadway, Missoula, MT 59802 (E-mail: duran@saintpatrick.org).

The costs of publication of this article were defrayed in part by the payment of page charges. The article must therefore be hereby marked “advertisement” in accordance with 18 U.S.C. Section 1734 solely to indicate this fact.

with five leads. Anesthesia was maintained with intermittent intravenously administered propofol and isoflurane at a gas level of 0.5–2.5% as needed. The heart was exposed with a standard left thoracotomy through the fourth intercostal space and a T-shaped incision of the pericardium. In preparation for cardiopulmonary bypass, a bolus injection of heparin (300 U/kg iv) was administered with a target activated clotting time of  $\geq 480$  s. The ascending aorta was cannulated with a 16-Fr arterial cannula, and a 32-Fr dual-stage single venous cannula (Medtronic, Minneapolis, MN) was inserted into the right atrium. After initiation of cardiopulmonary bypass, a LV vent was inserted through the LV apex. After the ascending aorta was cross-clamped, cold blood cardioplegia was infused into the aortic root.

Eleven 2-mm ultrasonic crystals (Sonometrics, London, Ontario, Canada) were implanted and secured with 5-0 polypropylene sutures at the mitral valve annulus at the midpoint of the posterior mitral annulus (PMA), the lateral mitral annulus [anterolateral (P1) and posterolateral (P2)], both fibrous trigones [anterior (T1) and posterior (T2)], the lowest endoluminal point of the right coronary sinus (RCS), both papillary muscle tips [anterolateral (M1) and posteromedial (M2)], the anterior LV endocardial wall between the tips of the papillary muscles (AW), the septal LV endocardial wall at the level of the papillary muscle tips (SW), and the LV apex. In addition, 1-mm crystals were placed at the midpoint of the free margin of the anterior and posterior leaflets (AL and PL, respectively; Fig. 1).

All endocardial electrodes of the crystals, except those corresponding to the papillary muscle tips (AW and SW) and apex, were exteriorized through the left atriotomy. The papillary muscle and apex electrodes were exteriorized through the apex, and the crystal in the RCS was exteriorized through an aortotomy. A high-fidelity, catheter-tipped pressure transducer (model 510, Millar Instruments, Houston, TX) was placed within the lumen of the proximal ascending aorta and in the LV cavity through the apex. A flowmeter (model T206, Transonic Systems, Ithaca, NY) ring was placed around the ascending aorta. After the animals were weaned from cardiopulmonary bypass,

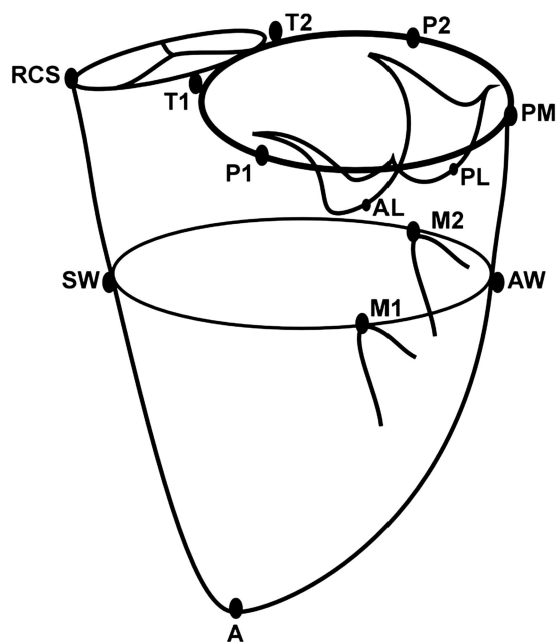


Fig. 1. Crystal locations. A, apex; SW, endocardial septal wall; AW, endocardial anterior wall; M1, anterolateral papillary muscle tip; M2, posteromedial papillary muscle tip; RCS, right coronary sinus; T1, anterior trigone; T2, posterior trigone; P1, anterolateral mitral annulus; P2, posterolateral mitral annulus; PMA, midpoint of posterior mitral annulus; AL, tip of anterior mitral leaflet; PL, tip of posterior mitral leaflet.

Table 1. Hemodynamic parameters

Hemodynamic Parameter	Baseline
Heart rate, beats/min	108.7 $\pm$ 5.8
Central venous pressure, mmHg	10.2 $\pm$ 0.6
Systolic pulmonary arterial pressure, mmHg	24.8 $\pm$ 2.2
Mean pulmonary arterial pressure, mmHg	17.0 $\pm$ 1.2
Diastolic pulmonary arterial pressure, mmHg	12.7 $\pm$ 1.4
Left atrial pressure, mmHg	9.3 $\pm$ 0.5
Left ventricular systolic pressure, mmHg	95.5 $\pm$ 4.5
Left ventricular end-diastolic pressure, mmHg	14.8 $\pm$ 2.5
Stroke volume, ml	44.5 $\pm$ 4.7

Values are means  $\pm$  SE.

the venous and arterial cannulas were removed, and the heparin was neutralized with protamine. The pericardium was closed with a 3-0 polypropylene suture. Recordings were obtained after the animal was hemodynamically stable ( $\geq 30$  min after the animal was weaned from cardiopulmonary bypass) to ensure the presence of normal loading conditions.

**Definition of the phases of the cardiac cycle.** Geometric changes were time related to each phase of the cardiac cycle defined from the aortic and LV pressure curves. The end of diastole was defined as the point of increasing LV pressure trace ( $dP/dt > 0$ ). The end of IVC was defined as the beginning of ejection at the crossing point of the LV and aortic pressure curves (LV pressure/aortic pressure = 0). The dicrotic notch in the aortic pressure curve defined end ejection. The end of IVR, or the initial phase of diastole, was defined by the mitral valve opening determined by the initial separation of the crystals located in the leaflets' free edge (AL–PL) (7).

**Definition of anatomic regions.** Longitudinal axes were defined as distances between the apex and the base of the aortic valve RCS, the fibrous trigones (T1 and T2), the lateral mitral annulus (P1 and P2), and the PMA. Movements of the mitral valve were recognized by the changes in distance between the crystals on the AL and PL.

Transverse diameters were defined as the distance between SW and AW and the distance between the crystals on M1 and M2 (Fig. 1).

**Data acquisition.** Distances between crystals were measured with a digital ultrasonic measurement system (TRX series, Sonometrics) using 13 transmitter/receiver crystals. A postprocessing program (Sonometrics) was used for examination of each individual distance between crystals and for three-dimensional reconstruction of the crystal coordinates. The data sampling rate was 200 Hz, with a time frame of  $\sim 5$  ms and smallest measurable change in distance of 0.024 mm, which allowed us to investigate distance changes during IVC and IVR.

Pressure transducer control units (model TCB 600, Millar Instruments) and Mikro-Tip pressure transducers (Millar Instruments) were used to obtain the LV and aortic pressures. Pulmonary and left atrial pressures were measured directly through a 20-gauge needle and a conventional pressure transducer. Aortic flow was recorded using an ultrasonic flow probe (models T206 and 20A, Transonic Systems) placed around the ascending aorta. Flow readings were used to calculate stroke volume. All distances, flows, and pressures were displayed and recorded simultaneously on the same screen by the Sonometrics system to ensure that all data were synchronized and recorded on the same time line. An effort was made to record the measurements under stable hemodynamic conditions of heart rate and loads with a closed pericardium.

**Measurement and statistical analysis methods.** Distances were explored in a coordinate-independent analysis, using only distance measurements (5). After close examination of the data, three consecutive heartbeats that contained the least amount of noise were chosen for analysis. The summary statistics are reported as means  $\pm$  SE. Normal distribution of measured data was rejected by Kolmogorov-Smirnov (Lilliefors) test. Therefore, data were tested by Wilcoxon's

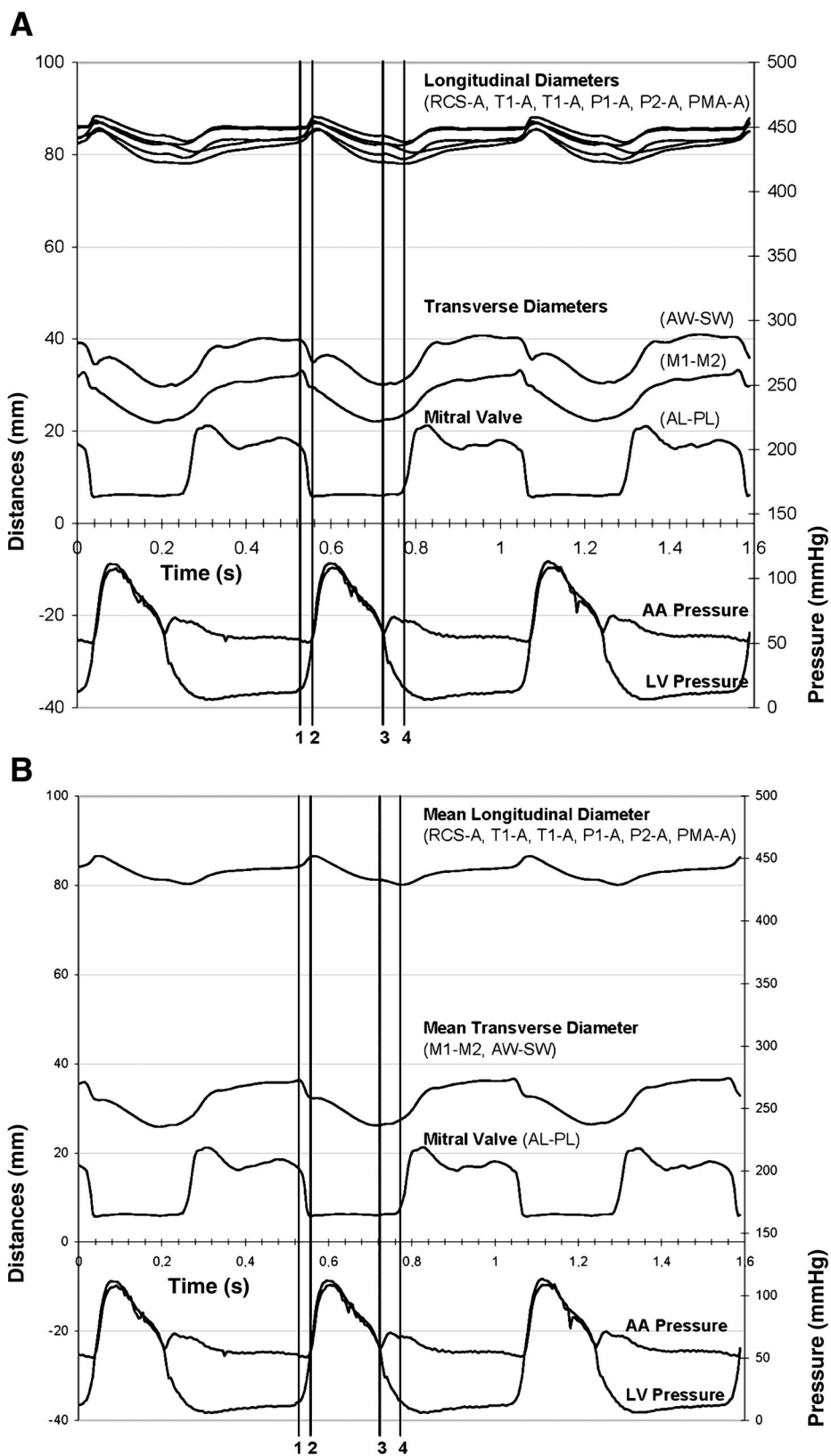


Fig. 2. *A*: phases of the cardiac cycle with changes in longitudinal and transverse diameters in 1 sheep. *B*: phases of the cardiac cycle with changes in mean longitudinal and transverse diameters in 1 sheep. 1, Beginning of isovolumic contraction; 2, beginning of ejection; 3, end of ejection; 4, end of isovolumic relaxation. AA pressure, aortic pressure.

Table 2. Time pattern

Phase	Time, ms
IVC	33 ± 3
Mitral valve closure after beginning of IVC	26 ± 3
Ejection	226 ± 20
IVR	56 ± 6
Diastole	250 ± 26

Values are means ± SE. IVC and IVR, isovolumic contraction and relaxation.

signed ranks test with a significance level of  $\alpha = 0.05$  using SPSS 11.0.1. for Windows (SPSS, Chicago, IL).

## RESULTS

All six sheep survived implantation of the sonomicrometric crystals (Fig. 1). Necropsy after death showed the crystals in the correct position. The hemodynamic parameters at the time of data acquisition are shown in Table 1. Sinus rhythm was present in all sheep after they were weaned from bypass.

**Mitral valve closure during IVC.** The mitral valve was open for the first three-quarters of IVC ( $33 \pm 3$  ms) and closed after  $26 \pm 3$  ms ( $77.60 \pm 4.32\%$  of IVC) at the beginning of the last quarter of IVC (Fig. 2A, Table 2).

**IVC.** At the beginning of IVC, while the mitral valve was still open, LV mean transverse diameter started to shorten by  $-26.16 \pm 4.55\%$  of its total expansion ( $9.33 \pm 1.23$  mm), with a fast decrease from  $95.55 \pm 1.80\%$  to  $69.39 \pm 3.99\%$  followed by a small notch at the beginning of ejection and a subsequent continuous shortening during systole (Fig. 2A). Simultaneously, during IVC, the mean longitudinal diameter increased by  $30.80 \pm 9.54\%$  of its total expansion ( $5.74 \pm 1.01$  mm), with a fast lengthening from  $64.21 \pm 3.76\%$  to  $95.01 \pm 1.28\%$ , reaching its peak precisely at the beginning of ejection and then shortening throughout the remainder of systole (Table 3).

**IVR.** LV mean transverse diameter reached maximum shortening of  $2.65 \pm 0.79\%$  of its total expansion ( $9.33 \pm 1.23$  mm) exactly at the end of ejection and started to expand by  $11.01 \pm 3.18\%$  of total expansion during IVR (Fig. 2A). The shortening in the LV longitudinal diameter during ejection reached a small plateau at the beginning of IVR and decreased further by  $-21.37 \pm 6.91\%$  of its total expansion ( $9.33 \pm 1.23$  mm) from  $24.43 \pm 7.16\%$  at end ejection to maximum shortening of

$3.06 \pm 0.86\%$  precisely when the mitral valve started to open (Table 4).

## DISCUSSION

**Mitral valve closure.** Contrary to the general opinion that the mitral valve closes at the very beginning of IVC, we found that it was still open at that moment. Our data show that the mitral valve is open during the first three-quarters of IVC. It closed at the beginning of the last quarter, confirming data presented previously by our group (14, 15) (Fig. 2B). Given that motion must be preceded by an acceleration phase and that acceleration in fluids is driven by pressure gradients, it makes sense that a pressure gradient must significantly precede the flow that closes the mitral valve. An instantaneous closure would only be possible with a weightless, incompressible fluid.

Yellin et al. (33) implanted a flow probe in the LV inflow tract and showed a negative flow at the mitral orifice during IVC. They interpreted this finding as an artifact, because they assumed that the mitral valve must already be closed at the onset of IVC. Also, finding that the first heart sound occurred during the rapid ventricular pressure development (or IVC), and not at end diastole as expected, they concluded that this sound was generated by the vibration of the already closed and tense mitral valve. Our data clearly show that the mitral valve remains open during most of IVC, while there is a rapid rise in LV pressure. As found by Yellin et al., some degree of regurgitation through the open mitral valve is likely. If this is so, the concept of an isovolumic phase is open to criticism. We can also probably assume that closure of the mitral valve at the last quarter of IVC contributes to the generation of the first heart sound, which occurs  $\sim 7$  ms before ejection (8, 12, 33). Therefore, it might be incorrect to define IVC as the interval between the start of LV rising pressure and the opening of the aortic valve. Furthermore, previous work in our laboratory showed that the aortic valve leaflets start to separate while a negative gradient still exists between the LV and the ascending aorta (13). Again, the concept of an isovolumic phase becomes doubtful.

**IVC phase.** On the basis of the early experiments of Rushmer et al. (23–25), it has been accepted that the LV becomes more spherical during IVC. This phenomenon is easily visible intraoperatively in the beating heart. Intracardially, we found the opposite pattern. During the initial phase of LV contraction, the endocardial shape of the LV became more elliptical (i.e., its

Table 3. IVC: phase-related changes at each phase of the cardiac cycle

Distance	Begin IVC (dt/dP > 0)	Begin Ejection ( $P_{LV}-P_{AA}=0$ )	Change of Distance During IVC	Total Expansion
M1–M2	28.13 ± 2.63	26.69 ± 2.46	-1.44 ± 0.28	7.50 ± 3.31*
AW–SW	37.29 ± 2.05	33.86 ± 1.55	-3.44 ± 0.36	11.17 ± 1.16*
Mean transverse diameter	32.71 ± 2.34	30.27 ± 2.02	-2.44 ± 0.46	9.33 ± 1.23*
RCS–A	92.81 ± 5.34	94.62 ± 5.41	1.81 ± 0.49	5.61 ± 0.81*
T1–A	92.43 ± 4.83	93.93 ± 4.83	1.49 ± 0.20	5.32 ± 0.75*
T2–A	89.03 ± 4.94	89.89 ± 4.88	0.87 ± 0.14	4.36 ± 0.78*
P1–A	88.37 ± 4.38	90.57 ± 4.54	2.20 ± 0.30	6.87 ± 0.84*
P2–A	81.99 ± 4.47	83.53 ± 4.40	1.54 ± 0.33	5.60 ± 0.74*
PMA–A	81.63 ± 5.14	84.50 ± 5.20	2.87 ± 0.36	6.67 ± 1.01*
Mean longitudinal diameter	87.71 ± 4.85	89.51 ± 4.93	1.79 ± 0.30	5.74 ± 0.82*

Values are means ± SE in mm. dP/dt, 1st derivative of pressure;  $P_{LV}$ , left ventricular pressure;  $P_{AA}$ , aortic pressure; A, apex; SW, endocardial septal wall; AW, endocardial anterior wall; M1, anterolateral papillary muscle tip; M2, posteromedial papillary muscle tip; RCS, right coronary sinus; T1, anterior trigone; T2, posterior trigone; P1, anterolateral mitral annulus; P2, posterolateral mitral annulus; PMA, midpoint of posterior mitral annulus. \* $\alpha < 0.05$ .

Table 4. *IVR: phase-related changes at each phase of the cardiac cycle*

Distance	End Ejection (dicrotic notch)	End of IVR (mitral valve opening)	Change of Distance During IVR	Total Expansion
M1–M2	21.16 ± 1.96	21.98 ± 2.03	0.82 ± 0.29	7.50 ± 3.31*
AW–SW	26.99 ± 2.01	28.29 ± 2.37	1.30 ± 0.84	11.17 ± 1.16*
Mean transverse diameter	24.07 ± 1.98	25.13 ± 2.20	1.06 ± 0.39	9.33 ± 1.23*
RCS–A	90.02 ± 5.05	89.46 ± 5.17	–0.55 ± 0.27	5.61 ± 0.81*
T1–A	89.92 ± 4.50	88.82 ± 4.58	–1.10 ± 0.30	5.32 ± 0.75*
T2–A	86.69 ± 4.64	85.93 ± 4.61	–0.77 ± 0.13	4.36 ± 0.78*
P1–A	85.32 ± 3.83	84.01 ± 4.00	–1.31 ± 0.35	6.87 ± 0.84*
P2–A	79.36 ± 4.10	78.45 ± 4.17	–0.91 ± 0.26	5.60 ± 0.74*
PMA–A	80.06 ± 4.61	78.39 ± 4.84	–1.67 ± 0.35	6.67 ± 1.01*
Mean longitudinal diameter	85.23 ± 4.45	84.18 ± 4.56	–1.05 ± 0.28	5.74 ± 0.82*

Values are means ± SE in mm. See Table 3 for definitions of abbreviations. \* $\alpha < 0.05$ .

longitudinal diameter increased while its transverse diameter decreased; Fig. 2*B*). This discrepancy is explained by the thickening of the LV wall during contraction (20, 31). This thickening results in an epicardial outward and an endocardial inward displacement and, consequently, a reduction in the LV endoluminal transverse diameter. According to Laplace's law (7), it can be hypothesized that this reduction in LV radius should reduce wall tension before ejection. The LV longitudinal diameter lengthened during IVC. As described by Robinson and associates (21), this longitudinal fiber stretch stores elastic kinetic energy that will be supplied during the beginning of longitudinal shortening.

**IVR phase.** We found no relaxation of the entire ventricle during IVR. After ejection, from closure of the aortic valve until opening of the mitral valve, both valves are firmly closed, and LV volume does not change. However, during this time, while the LV transverse diameter starts to increase, the longitudinal diameter continues to shorten (Fig. 2*B*). Our results are different from those of Nikolic et al. (18), who described a change in LV to an elliptical shape. Again, these dimensional measurements were done with epicardial sonomicrometric markers after mitral valve replacement and, presumably, with the deleterious effects that follow transection of all mitral valve chords (34). Our findings confirm the observations of Rankin et al. (20), who described a change in LV geometry to a spherical shape during the initial isovolumic phase of diastole in the direction opposite that observed during IVC. LV transverse diameter reaches its shortest distance (end of transverse contraction) exactly at the time of closure of the aortic valve and lengthens during IVR. LV longitudinal diameter shortens during systole. After a small plateau corresponding to aortic valve closure, LV endocardial longitudinal diameter continues to shorten during the entire IVR until the exact time of mitral valve opening. Consequently, to term this period relaxation is incorrect, because LV contraction and blood volume redistribution are still occurring. As demonstrated by Ashikaga et al. (1), endocardial sheet shortening occurs during IVR and appears to drive global torsional recoil to aid early diastolic filling.

The predominant paradigm that is used to understand the LV pump function with staccato mechanical parameters should probably be shifted toward a smoother, flow-directed behavior. Recent cardiac flow dynamic studies with three-dimensional MRI velocity mapping (11) and studies on LV mechanics (2–4, 28, 30), anisotropic material properties of myocardium (17), and transmural myocardial deformations (31) might pro-

vide a more physiological and real understanding of the fluid continuum of the cardiac phases.

**Limitations of the study.** We are aware that our approach is simple, but the present technology of high-resolution sonomicrometry requires that the number of sonomicrometry crystals be limited to a minimum. Sonomicrometry gives the distance between identical locations with high resolution (200 Hz) and a time frame of 5 ms, making it possible to investigate distance changes during IVC and IVR.

Pictorial methods, such as echocardiography and computed tomography scan, cannot precisely pursue a moving location over several slides; therefore, it is impossible for these methods to give precise distances between two moving points. Additionally, the time frame resolution of these methods is considerably longer (>30 ms). Cinefluoroscopy (29) with a high-speed camera or ultrafast MRI (6, 22) with true myocardial motion tracking makes it possible to observe the same location during IVC and IVR within 30–60 ms, but these techniques are still experimental. Sonomicrometry is a well-known and established technology.

In this experimental setting, it was impossible to address the rotational motion of the LV, which is essential for understanding LV function. Sonomicrometry allows precise, high-resolution recording of distances, but it cannot distinguish between active contraction and passive reshaping of the myocardium.

The sonomicrometric crystals and their electrodes might have interfered with the normal movements of the different structures. Also, the location of the crystals might vary between animals. To diminish this possibility, all surgeries were performed by the same surgeon.

All data were acquired in an acute, anesthetized, open-chest animal after cardiopulmonary bypass and cardioplegia and with the pericardial cavity surgically closed in all animals. Hemodynamic stability was carefully monitored, and the loading conditions were controlled. Despite this nonphysiological condition, the changes were very consistent among all animals. Additionally, findings in sheep are not necessarily applicable to humans.

**Conclusions.** Our findings from this study are as follows: 1) The mitral valve remains open during three-quarters of the IVC phase. 2) During IVC, the LV endoluminal transverse diameter decreases while its longitudinal diameter increases, resulting in an elliptical shape. 3) During IVR, the LV endoluminal longitudinal diameter continues to shorten as it does during ejection. Simultaneously, the LV transverse diameter increases from its shortest at end ejection. The LV acquires a more spherical

shape. 4) The concept of IVC and IVR phases might need to be revised.

#### ACKNOWLEDGMENTS

We appreciate the technical assistance of Leslie Trail, Lorinda Smith, and Holly Meskimen in the animal laboratory and the editorial assistance of Jill Roberts.

Present addresses of W. A. Goetz and H.-S. Lim: Nanyang Technological University, School of Mechanical and Aerospace Engineering, Singapore 639798. Present address of E. Lansac: Chirurgie Thoracique et Cardiovasculaire, Hopital Pitie-Salpetriere, Paris 75013, France.

#### GRANTS

W. A. Goetz was supported by a grant from Deutsche Forschungsgemeinschaft (Bonn, Germany) and the Max Kade Foundation (New York, NY). H.-S. Lim was supported by Singapore Ministry of Education and Nanyang Technological University Grant ARC 13/96.

#### REFERENCES

- Ashikaga H, Criscione JC, Omens JH, Covell JW, and Ingels NB Jr. Transmural left ventricular mechanics underlying torsional recoil during relaxation. *Am J Physiol Heart Circ Physiol* 286: H640–H647, 2004.
- Costa KD, Hunter PJ, Rogers JM, Guccione JM, Waldman LK, and McCulloch AD. A three-dimensional finite element method for large elastic deformations of ventricular myocardium. I. Cylindrical and spherical polar coordinates. *J Biomech Eng* 118: 452–463, 1996.
- Costa KD, Hunter PJ, Wayne JS, Waldman LK, Guccione JM, and McCulloch AD. A three-dimensional finite element method for large elastic deformations of ventricular myocardium. II. Prolate spheroidal coordinates. *J Biomech Eng* 118: 464–472, 1996.
- Costa KD, Takayama Y, McCulloch AD, and Covell JW. Lamellar fiber architecture and three-dimensional systolic mechanics in canine ventricular myocardium. *Am J Physiol Heart Circ Physiol* 276: H595–H607, 1999.
- Dagum P, Timek TA, Green GR, Lai D, Daughters GT, Liang DH, Hayase M, Ingels NB Jr, and Miller DC. Coordinate-free analysis of mitral valve dynamics in normal and ischemic hearts. *Circulation* 102: III62–III69, 2000.
- Fischer SE, McKinnon GC, Scheidegger MB, Prins W, Meier D, and Boesiger P. True myocardial motion tracking. *Magn Reson Med* 31: 401–413, 1994.
- Fuster V, Wayne AR, and O'Rourke RA. Normal physiology of the cardiovascular system. In: *Hurst's The Heart* (10th ed.), edited by Fuster V. New York: McGraw-Hill, 2001, p. 63–94.
- Gitterman M and Lewkowicz M. The first heart sound during the isovolumetric contraction. *J Biomech* 20: 35–49, 1987.
- Hinds JE, Hawthorne EW, Mullins CB, and Mitchell JH. Instantaneous changes in the left ventricular lengths occurring in dogs during the cardiac cycle. *Fed Proc* 28: 1351–1357, 1969.
- Horwitz LD, Bishop VS, Stone HL, and Stegall HF. Continuous measurement of internal left ventricular diameter. *J Appl Physiol* 24: 738–740, 1968.
- Kilner PJ, Yang GZ, Wilkes AJ, Mohiaddin RH, Firmin DN, and Yacoub MH. Asymmetric redirection of flow through the heart. *Nature* 404: 759–761, 2000.
- Laniado S, Yellin EL, Miller H, and Frater RW. Temporal relation of the first heart sound to closure of the mitral valve. *Circulation* 47: 1006–1014, 1973.
- Lansac E, Lim HS, Shomura Y, Lim KH, Rice NT, Goetz W, Acar C, and Duran CM. A four-dimensional study of the aortic root dynamics. *Eur J Cardiothorac Surg* 22: 497–503, 2002.
- Lansac E, Lim KH, Shomura Y, Goetz WA, Lim HS, Rice NT, Saber H, and Duran CMG. Dynamic balance of the aortomitral junction. *J Thorac Cardiovasc Surg* 123: 911–918, 2002.
- Lansac E, Lim KH, Shomura Y, Lim HS, Goetz WA, Stevens S, Oury JH, Acar C, and Duran CMG. Timing of mitral valve closure: the myth of the isovolumic contraction (Abstract). *J Am Coll Cardiol* 39: 431A, 2002.
- Lynch PR and Bove AA. Geometry of the left ventricle as studied by a high-speed cineradiographic technique. *Fed Proc* 28: 1330–1333, 1969.
- MacKenna DA, Omens JH, and Covell JW. Left ventricular perimysial collagen fibers uncoil rather than stretch during diastolic filling. *Basic Res Cardiol* 91: 111–122, 1996.
- Nikolic SD, Feneley MP, Pajaro OE, Rankin JS, and Yellin EL. Origin of regional pressure gradients in the left ventricle during early diastole. *Am J Physiol Heart Circ Physiol* 268: H550–H557, 1995.
- Pieper HP. Catheter-tip instrument for measuring left ventricular diameter in closed-chest dogs. *J Appl Physiol* 21: 1412–1416, 1966.
- Rankin JS, McHale PA, Arentzen CE, Ling D, Greenfield JC Jr, and Anderson RW. The three-dimensional dynamic geometry of the left ventricle in the conscious dog. *Circ Res* 39: 304–313, 1976.
- Robinson TF, Factor SM, and Sonnenblick EH. The heart as a suction pump. *Sci Am* 254: 84–91, 1986.
- Rogers WJ Jr, Shapiro EP, Weiss JL, Buchalter MB, Rademakers FE, Weisfeldt ML, and Zerhouni EA. Quantification of and correction for left ventricular systolic long-axis shortening by magnetic resonance tissue tagging and slice isolation. *Circulation* 84: 721–731, 1991.
- Rushmer RF. Initial phase of ventricular systole: asynchronous contraction. *Am J Physiol* 184: 188–194, 1956.
- Rushmer RF. Physical characteristics of myocardial performance. *Am J Cardiol* 18: 6–9, 1966.
- Rushmer RF and Crystal DK. Changes in configuration of the ventricular chambers during the cardiac cycle. *Circulation* 4: 211–218, 1951.
- Rushmer RF, Finlayson BL, and Nash AA. Movements of the mitral valve. *Circ Res* 4: 337–342, 1956.
- Salisbury PF, Cross CE, and Rieben PA. Phasic dimensional changes in the left ventricle. *Arch Int Physiol Biochim* 73: 188–208, 1965.
- Schmid P, Niederer P, Lunkenheimer PP, and Torrent-Guasp F. The anisotropic structure of the human left and right ventricles. *Technol Health Care* 5: 29–43, 1997.
- Tibayan FA, Rodriguez F, Langer F, Zasio MK, Bailey L, Liang D, Daughters GT, Ingels NB Jr, and Miller DC. Annular remodeling in chronic ischemic mitral regurgitation: ring selection implications. *Ann Thorac Surg* 76: 1549–1555, 2003.
- Torrent Guasp F. Agonist-antagonist mechanics of the descendent and ascendent segments of the ventricular myocardial band [in Spanish]. *Rev Esp Cardiol* 54: 1091–1102, 2001.
- Waldman LK, Nosan D, Villarreal F, and Covell JW. Relation between transmural deformation and local myofiber direction in canine left ventricle. *Circ Res* 63: 550–562, 1988.
- Wiggers CJ. Studies on the consecutive phases of the cardiac cycle. 1. The duration of the consecutive phases of the cardiac cycle and the criteria for their precise determination. *Am J Physiol* 56: 415–438, 1921.
- Yellin EL, Nikolic S, and Frater RW. Left ventricular filling dynamics and diastolic function. *Prog Cardiovasc Dis* 32: 247–271, 1990.
- Yun KL, Fann JI, Rayhill SC, Nasserbakht F, Derby GC, Handen CE, Bolger AF, and Miller DC. Importance of the mitral subvalvular apparatus for left ventricular segmental systolic mechanics. *Circulation* 82: IV89–IV104, 1990.